

# Centralized Reward Agent for Knowledge Sharing and Transfer in Multi-Task Reinforcement Learning

Haozhe Ma<sup>1</sup>, Zhengding Luo<sup>2</sup>, Thanh Vinh Vo<sup>1</sup>, Kuankuan Sima<sup>1</sup>, Tze-Yun Leong<sup>1</sup>

<sup>1</sup>National University of Singapore

<sup>2</sup>Nanyang Technological University

haozhe.ma@u.nus.edu, luoz0021@e.ntu.edu.sg, votv@comp.nus.edu.sg,  
kuankuan\_sima@u.nus.edu, leongty@comp.nus.edu.sg

## Abstract

Reward shaping is effective in addressing the sparse-reward challenge in reinforcement learning by providing immediate feedback through auxiliary informative rewards. Based on the reward shaping strategy, we propose a novel multi-task reinforcement learning framework that integrates a centralized reward agent (CRA) and multiple distributed policy agents. The CRA functions as a knowledge pool, which aims to distill knowledge from various tasks and distribute it to individual policy agents to improve learning efficiency. Specifically, the shaped rewards serve as a straightforward metric to encode knowledge. This framework not only enhances knowledge sharing across established tasks but also adapts to new tasks by transferring meaningful reward signals. We validate the proposed method on both discrete and continuous domains, including the representative meta world benchmark, demonstrating its robustness in multi-task sparse-reward settings and its effective transferability to unseen tasks.

## 1 Introduction

Reinforcement learning (RL) has made significant progress across various domains, like robotics (Kober et al., 2013), gaming (Lample and Chaplot, 2017), autonomous vehicles (Aradi, 2020), signal processing (Luo et al., 2024), and large language models (Shinn et al., 2023; Ouyang et al., 2022). However, environments with sparse and delayed rewards remain a significant challenge, as the absence of immediate feedback hinders the agent from distinguishing the value of states and leads to aimless exploration (Ladosz et al., 2022). Reward Shaping (RS) has been proven to be an effective technique to address this challenge by providing additional dense and informative rewards (Sorg et al., 2010b,a). Concurrently, multi-task reinforcement learning (MTRL) is becoming increasingly important for its ability to share and transfer knowledge across tasks. In this context, the auxiliary rewards infused with task-specific information in RS offer a straightforward entry to distribute knowledge among different tasks. Therefore, we believe that integrating RS techniques into MTRL is a highly promising and intuitive direction to enhance the efficacy of multi-task system learning.

Presently, numerous MTRL algorithms involving knowledge transfer have been developed. Policy distillation methods identify and combine the commonalities across different policies (Rusu et al., 2016; Teh et al., 2017; Parisotto et al., 2016; Xu et al., 2024; Ma et al., 2024b, 2023); representation sharing methods extract and disseminate the common features or gradients among agents (Yang et al., 2020; D’Eramo et al., 2020; Sodhani et al., 2021); and parameter sharing methods design architectural modules to reuse parameters or

layers across networks (Sun et al., 2022; Cheng et al., 2023). Despite their potential, these strategies often encounter challenges such as slow adaptation and response to the transferred knowledge, or suffer from delays in reutilizing and comprehending this information. Therefore, leveraging the RS mechanism, which directly adds a metric to the reward function, offers a compelling alternative to address these limitations.

Regarding the RS techniques, not all shaped rewards serve effectively as the medium for knowledge transfer. Specifically, the intrinsic motivation based rewards are typically designed using heuristics to generate task-agnostic signals. Examples include incorporating exploration bonuses (Bellemare et al., 2016; Ostrovski et al., 2017; Devidze et al., 2022), rewarding novel states (Tang et al., 2017; Burda et al., 2018), and encouraging curiosity-driven behaviors (Pathak et al., 2017; Mavor-Parker et al., 2022). Although these approaches broaden extensive exploration, they are not directly related to specific tasks and thus lack transferability. Consequently, we focus on another branch of RS methods, the task-contextual rewards, which automatically learn and encode task-specific information, such as the hidden values, contributions of states, or future-oriented insights, that can be shared effectively across various tasks (Ma et al., 2024a, 2025b,a; Mguni et al., 2023; Memarian et al., 2021).

To share task-related knowledge in MTRL via RS techniques, and inspired by the *ReLara* framework (Ma et al., 2024a), which integrates an assistant reward agent to densify sparse environmental rewards, we propose the **C**entralized Reward Agent based MTRL **f**RAMework (**CenRA**). The framework consists of two main components: a *centralized reward agent* (CRA) and multiple distributed *policy agents*. Each policy agent individually learns control behaviors within their respective tasks and shares their experiences with the CRA. The CRA extracts common knowledge from these experiences and learns to generate dense rewards that are encoded with task-specific information. These rewards are then distributed back to the policy agents to augment their original environmental rewards. Additionally, given that different tasks may contribute variably to the MTRL system, we introduce an information synchronization mechanism to further balance the knowledge distribution, considering task similarity and agent learning progress, to ensure a system-wide optimal performance. The main contributions of this paper are summarized as follows:

- (i) We propose the CenRA framework targeted to solve MTRL problems. It incorporates a CRA that functions as a centralized knowledge pool, efficiently distilling and distributing valuable information from various tasks to policy agents, and further adapting to new tasks.
- (ii) CenRA leverages the advantage of reward shaping techniques to infuse insights via dense rewards. This approach not only provides a direct metric for policy agents to absorb knowledge but also effectively addresses the sparse-reward challenge.
- (iii) We introduce an information synchronization mechanism that considers both task similarity and agent convergence progress to balance multi-task learning. This mechanism provides a novel direction for maintaining system equilibrium in MTRL.
- (iv) CenRA is validated in both discrete and continuous control MTRL environments, where the extrinsic rewards are sparse. CenRA outperforms several baseline models in terms of learning efficiency, knowledge transferability, and system-wide performance.

## 2 Related Work

Multi-task reinforcement learning (MTRL) has attracted significant attention recently due to its potential to share knowledge across multiple tasks, thereby improving learning performance (Caruana, 1993). We discuss existing MTRL literature from three main directions:

**Knowledge Transfer** methods focus on identifying and transferring task-relevant features across diverse tasks (Zeng et al., 2021). Policy distillation (Rusu et al., 2016) is a well-studied approach to extract and share task-specific behaviors or representations that many works are built on: Teh et al. (2017) introduced *Distral*, which distills a centroid policy from multiple task-policies; Parisotto et al. (2016) developed

*Actor-Mimic*, where a single policy is trained to mimic several expert policies from different tasks; while Yin and Pan (2017) incorporated hierarchical prioritized experience replay buffer to select and learn multi-task experiences; Hessel et al. (2019) further proposed an adaptation mechanism to equalize the impact of each task in policy distillation. Additionally, Xu et al. (2020) explored the transfer of offline knowledge to train policies, and further leveraged online learning for fine-tuning. Bai et al. (2023) introduced a dual-phase learning approach, optimizing individual policies while correcting them across multiple tasks. Mysore et al. (2022) used separate critics for each task to accompany a single actor to integrate their feedback. These methods mitigate gradient interference to an extent, however, balancing the distribution of knowledge across tasks is crucial. Without a careful trade-off, the performance of the entire system could be compromised.

**Representation Sharing** methods explore architectural solutions of reusing network modules or representing commonalities to the MTRL problem (D’Eramo et al., 2020; Devin et al., 2017; Hong et al., 2021). Sun et al. (2022) used a parameter compositional approach to learn and share a subspace of parameters, allowing policies for various tasks to be interpolated within it. Yang et al. (2020) employed soft modularization to learn foundational policies and utilized a routing network to generate probabilities to combine them. He et al. (2024) introduced the Dynamic Depth Routing framework, which dynamically adjusts the use of network modules in response to task difficulty. Sodhani et al. (2021) leveraged task-related metadata to create composable representations. Cheng et al. (2023) and Lan et al. (2023) both incorporated attention mechanisms: the former employed attention-based mixture of experts to capture task relationships, while the latter used Temporal Attention for contrastive learning purposes. Although these methods demonstrate efficacy in learning shared representations, they may struggle to fully capture the complexity of highly diverse tasks. Moreover, adapting shared structures to new tasks typically requires extra design efforts.

**Single-Policy Generalization** methods learn a single policy to solve multiple tasks simultaneously or continuously, in the absence of information from prior policies or task-specific details, in which case, the primary goal is to enhance the policy’s generalization capabilities. Model-free meta-learning techniques have been proposed to enhance the multi-task generalization (Finn et al., 2017). Yang et al. (2017) designed a sharing network structure that allows an agent to learn multiple tasks concurrently. Vuong et al. (2019) introduced a confidence-sharing agent to detect and define shared regions between tasks to support single policy learning. Wan et al. (2020) proposed a transfer learning framework to handle mismatches in state and action spaces. Additionally, several methods focus on overcoming gradient interference to enhance the generalization in various tasks (Chen et al., 2018; Yu et al., 2020a), while Ammar et al. (2014) developed a consecutive learning policy gradient approach. These methods are efficient in saving computational resources, but the generalization ability of the policy may be constrained when faced with out-of-distribution or previously unseen tasks.

### 3 Preliminaries

**Markov Decision Process (MDP)** models sequential decision-making problems under uncertainty. An MDP represents the interaction between an agent and its environment as a tuple  $\langle S, A, P, R, \gamma \rangle$ , where  $S$  is the state space,  $A$  is the action space,  $P : S \times A \times S \rightarrow [0, 1]$  is the probability of transiting from one state to another given an action,  $R : S \times A \rightarrow \mathbb{R}$  is the reward function, and  $\gamma \in [0, 1]$  is the discount factor to modulate the importance of future versus immediate reward.

**Multi-Task Reinforcement Learning (MTRL)** addresses the challenge of learning multiple tasks simultaneously within an integrated model to leverage commonalities and differences across tasks. Typically, MTRL introduces a task space  $\mathcal{T}$ , assuming all tasks are sampled from this space and thus follow a unique distribution. Each task is modeled as an independent MDP. An MTRL agent aims to learn optimal policies  $\pi_i : S \rightarrow A$  for each task  $T_i \sim \mathcal{T}$ , to maximize their corresponding expected cumulative rewards, or returns, denoted by  $G_i = \mathbb{E}[\sum_{t=0}^{\infty} \gamma^t R_i(s_t, a_t)]$ .

**RL with an Assistant Reward Agent (ReLara)** (Ma et al., 2024a) introduces a dual-agent framework designed to tackle the challenge of sparse rewards in RL. The operational architecture of ReLara is shown in Figure 1. Within this framework, the original agent is termed as *policy agent*, while an assistant *reward agent* is integrated to enrich the feedback mechanism by generating dense, informative rewards. The reward agent, trained as a self-contained RL agent, autonomously extracts hidden value information from the environmental states (and potentially the actions of the policy agent) to craft meaningful reward signals. These signals significantly improve learning efficiency by providing immediate and pertinent bonuses.

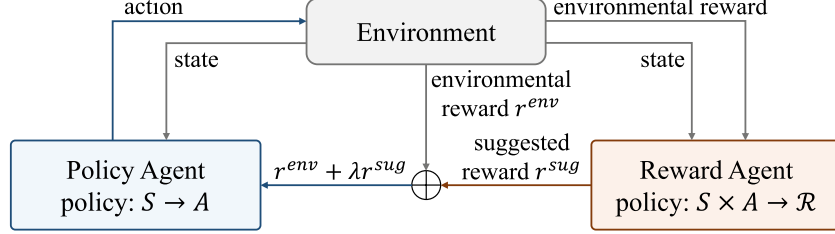


Figure 1: The ReLara framework Ma et al. (2024a).

## 4 Methodology

We propose **C**entralized Reward Agent **f**RAMework (**CenRA**) for MTRL, which incorporates a *centralized reward agent* (CRA) to support simultaneous reinforcement learning agents across multiple tasks. A high-level illustration of the CenRA framework is shown in Figure 2. The CRA is responsible for extracting general task-specific knowledge from various tasks and distributing valuable information to the policy agents by reconstructing their reward models. The detailed methodology for knowledge extraction and sharing is introduced in Section 4.1. Furthermore, to mitigate the potential disparities in the information that each task could contribute, which might lead to an imbalance in knowledge distribution, we introduce an information synchronization mechanism by considering two main factors: the similarity of the tasks and the online learning performance of the policy agents, details given in Section 4.2. Finally, the overall framework of CenRA is presented in Section 4.3.

### 4.1 Knowledge Extraction and Share

#### 4.1.1 Problem Formulation

We consider an MTRL setting comprising  $N$  distinct tasks  $\{T_1, T_2, \dots, T_N\}$ , all executed within the same type of environment  $\mathcal{E}$ . We assume that the shape of state  $s \in S$  and action  $a \in A$  remain uniform across tasks, to ensure the CRA processes consistent inputs. Despite this uniformity, each task may feature different state spaces, action spaces, goals, and transition dynamics. For instance, a series of mazes with the same size but varying map configurations would satisfy this condition. For each task  $T_i$ , we denote the transition function as  $P_i(s'|s, a)$  and the reward function as  $R_i(s, a)$ .

The centralized reward agent (CRA) is denoted as  $\mathcal{A}^{rd}$  and multiple policy agents are denoted as  $\{\mathcal{A}_1^{pol}, \mathcal{A}_2^{pol}, \dots, \mathcal{A}_N^{pol}\}$ . Each policy agent  $\mathcal{A}_i^{pol}$  operates independently to complete its corresponding task  $T_i$ , utilizing appropriate RL algorithms as backbones. For example, implementing DQN (Mnih et al., 2015) for discrete control tasks, while TD3 (Fujimoto et al., 2018) or SAC (Haarnoja et al., 2018a) for continuous control tasks. Moreover, the policy of CRA  $\mathcal{A}^{rd}$  is  $\pi^{rd}$ , and the internal policy of policy agent  $\mathcal{A}_i^{pol}$  is  $\pi_i^{pol}$ , respectively.

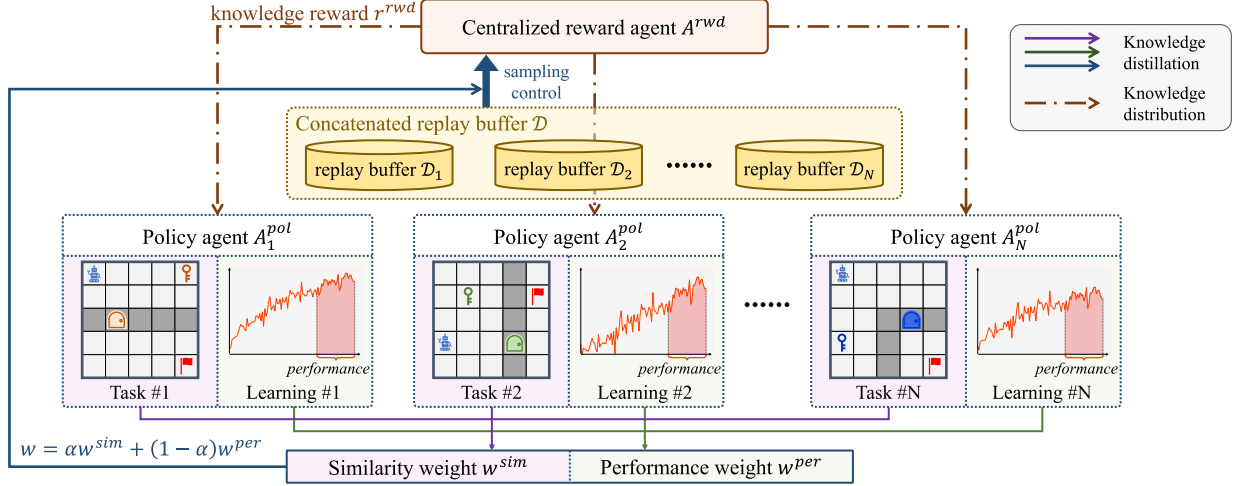


Figure 2: A high-level illustration of the CenRA framework.

#### 4.1.2 Centralized Reward Agent

The CRA  $\mathcal{A}^{rwd}$  aims to extract environment-relevant knowledge and distribute it to policy agents by generating additional dense rewards to support their original reward functions. Similar to the ReLara framework Ma et al. (2024a), we model the CRA as a self-contained RL agent, yet, as an extension to ReLara, our CRA is designed to concurrently interact with multiple policy agents and their respective tasks. The CRA’s policy  $\pi^{rwd}$  generates continuous rewards given both an environmental state and a policy agent’s behavior. Specifically,  $\pi^{rwd}$  maps the Cartesian product of the state space and action space,  $\mathcal{S} \times \mathcal{A}$ , to a defined *reward space*, which constrains the rewards to a range of real numbers,  $\mathcal{R} = [R_{min}, R_{max}] \subset \mathbb{R}$ . For simplicity’s sake, we denote the observation of CRA as  $s^{rwd} = (s_i, a_i)$ , where  $s_i \sim T_i$  and  $a_i \sim \pi_i^{pol}(s_i)$ . To distinguish from the environmental reward, the generated reward is termed as *knowledge reward*, denoted as  $r^{knw}$ .

We adopt an off-policy actor-critic algorithm to optimize the CRA Konda and Tsitsiklis (1999). To aggregate and reuse experiences from all policy agents, a concatenated replay buffer  $\mathcal{D} = \bigcup_{i=1}^N \mathcal{D}_i$  is constructed, where  $\mathcal{D}_i$  represents the replay buffer of each policy agent  $\mathcal{A}_i^{pol}$ . Besides, each transition is augmented with the CRA-generated knowledge reward,  $r^{knw}$ . Specifically, the transition from policy agent  $\mathcal{A}_i^{pol}$  stored in the replay buffer is defined as  $\tau = (s_t^{rwd}, r_t^{knw}, r_t^{env}, s_{t+1}^{rwd} | T_i)$ . The augmented transition includes all necessary information for optimizing both the CRA and each corresponding policy agent, thus making the concatenated replay buffer a shared resource across the entire framework and minimizing storage overhead.

The CRA’s update process involves using these stored transitions to optimize the reward-generating actor  $\pi^{rwd}$  and the value estimation critic. The objective function for the critic module is:

$$J(V^{rwd}) = \mathbb{E}_{\tau_t \sim \mathcal{D}} [\delta_t^2], \quad \delta_t = r_t^{env} + \gamma V^{rwd}(s_{t+1}^{rwd}) - V^{rwd}(s_t^{rwd}) | T_i, \quad (1)$$

where  $\tau_t = (s_t^{rwd}, r_t^{env}, s_{t+1}^{rwd} | T_i) \sim \mathcal{D}$ . Concurrently, the actor module is updated through the following objective function:

$$J(\pi^{rwd}) = \mathbb{E}_{\tau_t \sim \mathcal{D}} \left[ \mathbb{E}_{r_t^{knw} \sim \pi^{rwd}(\cdot | s_t^{rwd})} [\log \pi^{rwd}(r_t^{knw} | s_t^{rwd}) \cdot \delta_t] \right]. \quad (2)$$

### 4.1.3 Policy Agents with Knowledge Rewards

Each policy agent  $\mathcal{A}_i^{pol}$  interacts with its specific environment and stores the experiences in its corresponding replay buffer  $\mathcal{D}_i$ . Policy agents receive two types of rewards: the environmental reward  $r_i^{env}$  from their respective task  $T_i$  and the knowledge reward  $r^{knw}$  from CRA. The augmented reward is given by:

$$r_i^{pol} = r_i^{env} + \lambda r^{knw}, \quad r^{knw} \sim \pi^{rwd}(\cdot | s_i, a_i), \quad (3)$$

where  $\lambda \in (0, 1]$  is a scaling weight factor. The optimal policy  $\pi_i^{pol*}$  for each agent is derived by maximizing the cumulative augmented reward:

$$\pi_i^{pol*} = \arg \max_{\pi_i^{pol}} \mathbb{E}_{(s_i, a_i) \sim \pi_i^{pol}} \left[ \sum_{t=0}^{\infty} \gamma^t r_i^{pol} \right]. \quad (4)$$

It is worth noting that the environmental reward  $r_i^{env}$  is retrieved from the replay buffer (if adopting an off-policy approach). Conversely, the knowledge reward  $r^{knw}$  is computed in real-time using the most recently updated  $\mathcal{A}^{rwd}$ , ensuring it reflects the latest learning advancements. Lastly, each policy agent is able to employ any suitable RL algorithm, whether on-policy or off-policy, to best address its specific task, which enhances the CenRA framework’s generality and flexibility.

## 4.2 Information Synchronization of Policy Agents

In the CenRA framework, the information provided by different tasks may exhibit significant disparities, potentially leading to an imbalance in knowledge extraction and distribution. In this section, we introduce an information synchronization mechanism for CenRA to maintain a balanced manner from the perspective of the entire system. Specifically, this mechanism is implemented by controlling the quantity of samples that CRA retrieves from each task’s replay buffer  $\mathcal{D}_i$  by a *sampling weight*  $\mathbf{w}$ . We mainly consider two aspects: the similarity among tasks and the real-time learning performance of the policy agents.

**Similarity Weight** is derived from the similarity among tasks, enabling the CRA to focus on relatively outlier tasks. To simplify computation, we use the hidden layers extracted from each policy agent’s neural network encoders to represent the tasks’ features. To reduce randomness, we average the hidden features of the most recent  $K$  steps. We adopt a cross-attention mechanism, which is widely used in neural networks, to calculate the similarity weight Vaswani et al. (2017). Specifically, for task  $T_i$ , let  $\mathbf{H}_i$  denote the averaged hidden feature vector, which serves as the *key*, and the centroid of all tasks  $\mathbf{c}$  acts as the *query*. Then, the similarity  $s_i$  of task  $T_i$  to the centroid of the task cluster is calculated as:

$$s_i = \frac{\mathbf{c}^T \cdot \mathbf{H}_i}{\sqrt{D}}, \quad \mathbf{c} = \frac{1}{N} \sum_{k=1}^N \mathbf{H}_k, \quad (5)$$

where  $D$  is the dimension of the hidden feature to prevent gradient vanishing or exploding. A larger  $s_i$  indicates a greater similarity between  $T_i$  and the centroid. Given our assumption is that the tasks farther from the centroid require more attention, the *similarity weight* is defined as  $\mathbf{w}^{sim} = \text{Softmax}([1/s_1, 1/s_2, \dots, 1/s_N])$ .

**Performance Weight** is determined by the real-time learning performance of each policy agent, to ensure the CRA focuses more on lagging tasks. Similar to the similarity weight, we average the environmental rewards  $r_i^{env}$  from the most recent  $K$  steps, denoted as  $R_i^{tail}$ , to measure the recent learning trends. The *performance weight* is then defined as  $\mathbf{w}^{per} = \text{Softmax}([1/R_1^{tail}, 1/R_2^{tail}, \dots, 1/R_N^{tail}])$ .

Lastly, the final *sampling weight*  $\mathbf{w}$  combines the similarity weight and the performance weight as  $\mathbf{w} = \alpha \mathbf{w}^{sim} + (1 - \alpha) \mathbf{w}^{per}$ , where  $\alpha$  is a hyperparameter to balance the two aspects. The CRA samples from each replay buffer  $\mathcal{D}_i$  according to  $\mathbf{w}$ , ensuring a balanced and effective knowledge extraction and learning.

### 4.3 Overall Framework

The overall framework of CenRA is summarized in Algorithm 1. The CRA and policy agents are updated alternately and asynchronously, with the frequency of updating the CRA adjustable according to the actual situation. Sampling weights are calculated in real-time, using the most recently optimized encoders and the current learning performance, ensuring CRA continuously adjusts its focus to optimally balance knowledge extraction across multiple tasks.

The learned CRA acts as a robust knowledge pool, which is able to support new tasks as an additional module by transferring knowledge through auxiliary reward signals. This is particularly beneficial in sparse-reward environments, as the knowledge rewards can guide the policy agents toward the correct direction and reduce the exploration burden. Additionally, the CRA can be further optimized alongside new tasks in a continuous learning scheme that enhances adaptability and effectiveness in dynamic settings.

---

**Algorithm 1** Centralized Reward Agent based MTRL

---

**Require:** Multiple tasks  $\{T_1, T_2, \dots, T_N\}$ .  
**Require:** Policy agents  $\{\mathcal{A}_1^{pol}, \mathcal{A}_2^{pol}, \dots, \mathcal{A}_N^{pol}\}$ .  
**Require:** Centralized reward agent  $\mathcal{A}^{rwd}$ .  
**Require:** Concatenated replay buffer  $\mathcal{D} = \bigcup_{i=1}^N \mathcal{D}_i$ .

- 1: **for** each iteration **do**
- 2:   **for** each task  $T_i$  **do**
- 3:      $(s_t, a_t, r_t^{env}, s_{t+1}, a_{t+1}) \sim \text{Interact}(\mathcal{A}_i^{pol}, T_i)$  ▷ Interact and collect one transition
- 4:      $r_t^{knw} \sim \mathcal{A}^{rwd}(s_t, a_t)$  ▷ Sample an off-policy knowledge reward
- 5:      $s_t^{rwd} = (s_t, a_t), s_{t+1}^{rwd} = (s_{t+1}, a_{t+1})$
- 6:      $\mathcal{D}_i \leftarrow \mathcal{D}_i \cup \{(s_t^{rwd}, r_t^{knw}, r_t^{env}, s_{t+1}^{rwd}) | T_i\}$  ▷ Store the transition in corresponding  $\mathcal{D}_i$
- 7:     Update policy agent  $\mathcal{A}_i^{pol}$  ▷ Update  $\mathcal{A}_i^{pol}$  using backbone RL algorithm
- 8:   **end for**
- 9:    $\mathbf{w} = \alpha \mathbf{w}^{sim} + (1 - \alpha) \mathbf{w}^{per}$  ▷ Calculate sampling weight
- 10:    $\{s_t^{rwd}, r_t^{knw}, r_t^{env}, s_{t+1}^{rwd} | T_i\}_{\mathcal{B}} \sim \mathcal{D} | \mathbf{w}$  ▷ Draw samples based on the sampling weight
- 11:   Update centralized reward agent  $\mathcal{A}^{rwd}$
- 12: **end for**

---

## 5 Experiments

We conduct experiments in four MTRL domains as shown in Figure 3: the widely used **Meta-World** benchmark (including **ML10** with 10 tasks and **ML50** with 50 tasks) (Yu et al., 2020b), **2DMaze**, **3DPickup** (Chevalier-Boisvert et al., 2024), and **MujocoCar** (Ji et al., 2023). All tasks, including those in Meta-World, are crafted to provide **sparse environmental rewards**, where the agent receives a reward of 1 only upon successful completion of the final objective, and 0 otherwise. The detailed task configurations are provided in Appendix A.

### 5.1 Comparative Evaluation in MTRL

We benchmark CenRA against several state-of-the-art baselines: (a) the backbone RL algorithms of the policy agents: DQN (Mnih et al., 2015) for discrete control tasks and SAC (Haarnoja et al., 2018b) for continuous control tasks; (b) the ReLara algorithm (Ma et al., 2024a), which can be regarded as a decentralized variant of CenRA, where each policy agent is paired with a separate reward agent, without cross-task information sharing; (c) the Policy Optimization and Policy Correction (PiCor) algorithm (Bai et al., 2023); (d) the Multi-Critic Actor Learning (MCAL) algorithm (Mysore et al., 2022); (e) the Parameter-compositional MTRL (PaCo) algorithm (Sun et al., 2022); and (f) the MTRL with Soft Modularization

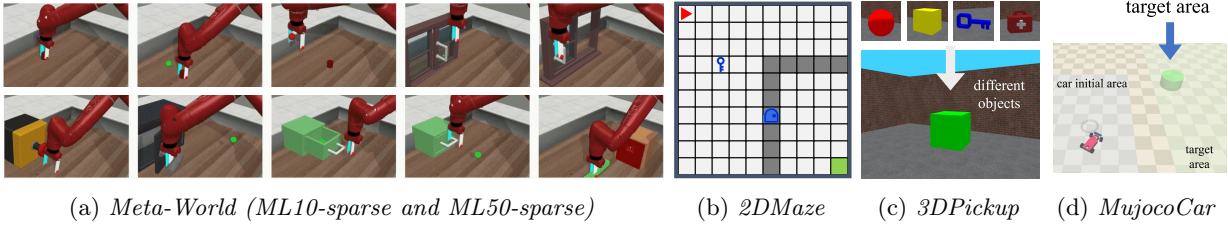


Figure 3: Environments with multiple tasks. (a) **Meta-World**: two sparse-reward versions are used: **ML10-sparse** and **ML50-sparse**, including diverse robotic manipulation tasks. (b) **2DMaze**: 2D maze tasks where the agent must pick up a key and then pass through a door to exit. (b) **3DPickup**: 3D maze tasks where the agent aims to navigate to and pick up different target objects at different locations. (c) **MujocoCar**: mujoco-based race car aims to navigate to different specified areas.

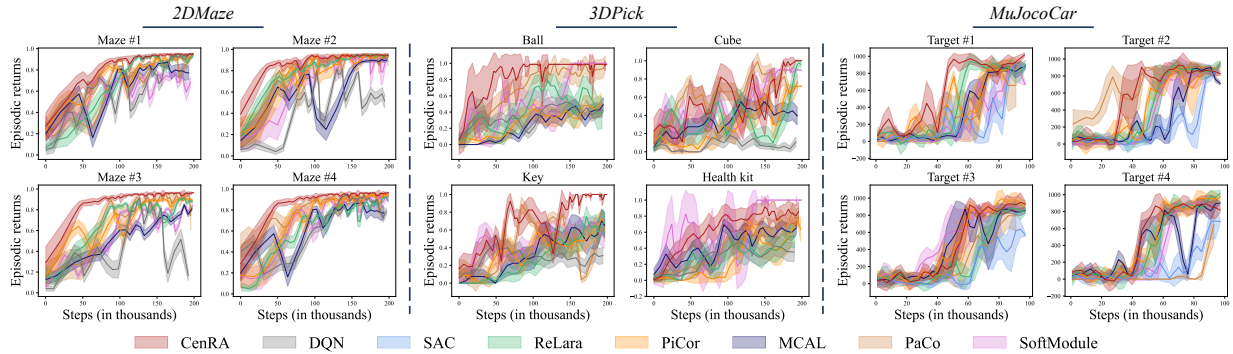


Figure 4: Comparison of CenRA with baselines in *2DMaze*, *3DPickup*, and *MujocoCar* domains.

(SoftModule) (Yang et al., 2020). They are implemented by either the *CleanRL* library (Huang et al., 2022) or official codebases. Each task is trained with 10 different random seeds, and the average results are reported.

In the *Meta-World* domain, *ML10-sparse* provides 10 training tasks and 5 held-out test tasks, while *ML50-sparse* includes 45 training tasks and 5 test tasks. For the remaining domains, each consists of 4 training tasks and 1 test task. In this section, we evaluate the final returns achieved by the trained agents, averaged over all training tasks in each domain, as shown in Table 1. We additionally report the episodic returns and their standard errors throughout training in the *2DMaze*, *3DPickup*, and *MujocoCar* domains in Figure 4. To ensure a fair comparison, we adopt consistent hyperparameters (where applicable) and identical network architectures across all experiments; detailed configurations are provided in Appendix B.

We observe that CenRA consistently outperforms all baselines in three main aspects. First, it achieves the highest episodic returns in all tasks, demonstrating superior learning efficiency and faster convergence. Moreover, it demonstrates good stability and robustness, exhibiting fewer fluctuations and oscillations, especially after convergence, compared to other models. Notably, all tasks provide only sparse rewards, CenRA addresses this challenge through the auxiliary dense rewards with meaningful information, effectively guiding learning. This mechanism not only distinguishes CenRA from other structurally shared methods, but also provides a targeted solution to the sparse-reward problem. Second, while baselines like PiCor and MCAL often show uneven progress across different tasks within the same domain, CenRA maintains well-balanced performance by showing relatively consistent learning progress and minimal variability across each four-task groups. This ensures that no single task dominates or lags behind, which is crucial in multi-task learning. Third, the CRA effectively enhances knowledge sharing among tasks. This is evident from the comparison with ReLara, which uses independent reward agents and lacks the mechanism for



Table 1: Episodic returns (mean  $\pm$  standard error) of all trained agents tested over 100 episodes and averaged across all training tasks in each domain ( $\uparrow$  higher is better).

Algorithm	<i>ML10-sparse</i>	<i>ML50-sparse</i>	<i>2DMaze</i>	<i>3DPickup</i>	<i>MujocoCar</i>
CenRA (ours)	<b>0.875 <math>\pm</math> 0.121</b>	<b>0.755 <math>\pm</math> 0.034</b>	<b>0.913 <math>\pm</math> 0.023</b>	<b>0.880 <math>\pm</math> 0.060</b>	<b>514.875 <math>\pm</math> 0.675</b>
DQN/SAC	0.256 $\pm$ 0.056	0.189 $\pm$ 0.012	0.645 $\pm$ 0.070	0.243 $\pm$ 0.048	198.000 $\pm$ 0.453
ReLara	0.674 $\pm$ 0.105	0.541 $\pm$ 0.057	0.803 $\pm$ 0.065	0.565 $\pm$ 0.088	429.800 $\pm$ 0.655
PiCor	0.865 $\pm$ 0.230	0.672 $\pm$ 0.123	0.818 $\pm$ 0.053	0.438 $\pm$ 0.085	437.550 $\pm$ 0.663
MCAL	0.842 $\pm$ 0.067	0.605 $\pm$ 0.055	0.885 $\pm$ 0.080	0.548 $\pm$ 0.068	369.200 $\pm$ 0.595
PaCo	0.854 $\pm$ 0.045	0.582 $\pm$ 0.022	0.834 $\pm$ 0.057	0.557 $\pm$ 0.072	421.210 $\pm$ 0.635
SoftModule	0.630 $\pm$ 0.042	0.423 $\pm$ 0.057	0.822 $\pm$ 0.076	0.486 $\pm$ 0.055	355.125 $\pm$ 0.594

knowledge exchange. By extracting and distributing insights from one task to another, the CRA improves the learning efficiency of individual tasks, highlighting the advantages of integrated knowledge management.

## 5.2 What Has the Centralized Reward Agent Learned?

In this section, we visualize the learned *knowledge rewards* by the centralized reward agent  $\mathcal{A}^{rd}$  in the *2DMaze* environment. After training on the four tasks in Section 5.1 of the paper, we let the CRA generate the knowledge rewards for each action in every state and visualize the action direction that yields the maximum rewards,  $a^* = \arg \max_a \pi^{rd^*}(s_i, a), s_i \sim S$ , in Figure 5.

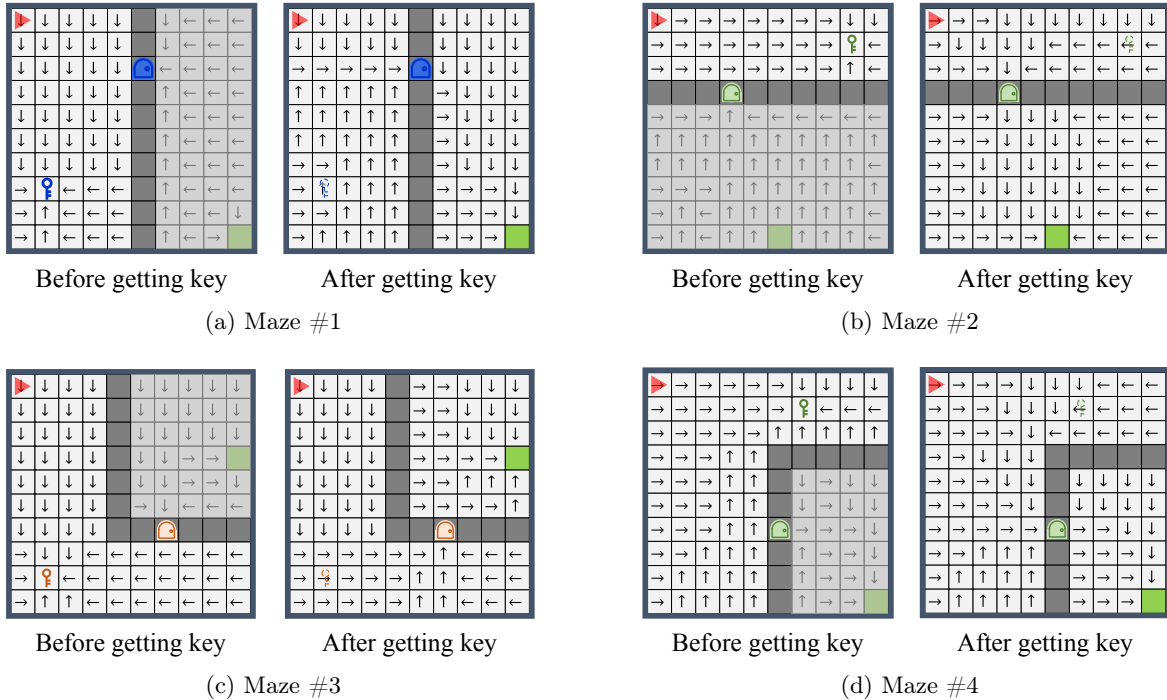


Figure 5: Visualization of the action yielding the maximum knowledge rewards in the four *2DMaze* tasks.

The shaded areas in the figures represent regions within the real task that the agent cannot reach, as it cannot access the space behind the door without picking up the key. However, we forced the agent into these areas for evaluation. Outside the shaded regions, we observe that the CRA successfully learned meaningful knowledge rewards. Before picking up the key, the agent received the highest reward in the corresponding state when moving towards the key. Similarly, after picking up the key, the agent received

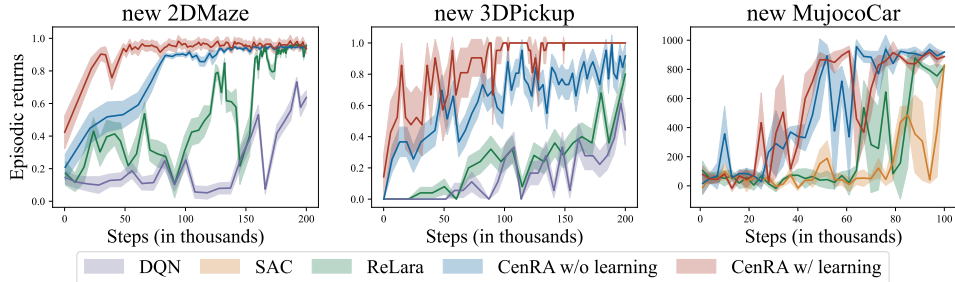


Figure 6: Comparison of the learning performance of CenRA with the baselines in new tasks.

Table 2: Episodic returns (mean  $\pm$  standard error) of all trained agents in the new tasks, tested over 100 episodes in each domain ( $\uparrow$  higher is better).

Algorithm	<i>ML10-sparse</i>	<i>ML50-sparse</i>	<i>2DMaze</i>	<i>3DPickup</i>	<i>MujocoCar</i>
CenRA w/ learning	<b>0.902 <math>\pm</math> 0.021</b>	<b>0.824 <math>\pm</math> 0.012</b>	<b>0.952 <math>\pm</math> 0.010</b>	<b>0.963 <math>\pm</math> 0.002</b>	<b>532.080 <math>\pm</math> 1.610</b>
CenRA w/o learning	0.887 $\pm$ 0.011	0.809 $\pm$ 0.009	0.894 $\pm$ 0.032	0.678 $\pm$ 0.003	524.727 $\pm$ 0.588
ReLara	0.702 $\pm$ 0.086	0.612 $\pm$ 0.012	0.759 $\pm$ 0.056	0.263 $\pm$ 0.002	224.648 $\pm$ 0.492
DQN/SAC	0.228 $\pm$ 0.105	0.210 $\pm$ 0.034	0.263 $\pm$ 0.084	0.158 $\pm$ 0.003	129.055 $\pm$ 0.296

the highest reward when moving towards the door and the final target. This demonstrates that in scenarios where the original environmental rewards are sparse, these detailed knowledge rewards can effectively guide the agent to converge more quickly.

### 5.3 Knowledge Transfer to New Tasks

In this section, we assess the CRA’s ability to transfer previously learned knowledge to unseen tasks. Specifically, we continue using the trained CRA model in Section 5.1, while initializing new policy agents to tackle new tasks from the same domain. These include 5 test tasks for *ML10-sparse* and *ML50-sparse*, and 1 test task for each of the remaining domains, none of which were encountered during the initial training. For the CenRA, we explore two scenarios: (1) the CRA continues to be optimized in collaboration with the new policy agent (CenRA w/ learning); and (2) only the policy agent is updated while the CRA remains fixed, relying only on its previously acquired knowledge (CenRA w/o learning). We compare the two settings against the backbone algorithms and ReLara. In ReLara, the reward agent is trained anew without pre-learned knowledge. The results are presented in Figure 6 and Table 2.

We observe that CenRA with further learning achieved rapid convergence, mainly due to the CRA’s ability to retain previously acquired knowledge while continuing to adapt to new tasks through ongoing optimization. Remarkably, even without any additional training, CenRA still outperforms both ReLara, which requires training a new reward agent, and the backbone algorithms, which lack additional information. This advantage stems from the CRA’s ability to encode and transfer environment-relevant knowledge, which can then be directly reused by new policy agents to guide their learning. Such knowledge transfer is particularly critical in our experiments involving challenging sparse-reward tasks. Without any external knowledge, learning would require extensive exploration. However, the CRA provides meaningful dense rewards that significantly accelerate the learning process, even during the initial phases.

To further demonstrate CenRA’s transferability, we select the *2DMaze* environment to visualize the knowledge provided by CRA when facing an unseen task. As shown in Figure 7, we plot the directions of actions that yield the maximum knowledge reward at each position, categorized into two scenarios: before and after obtaining the key. While some guidance in peripheral regions may appear slightly misaligned,

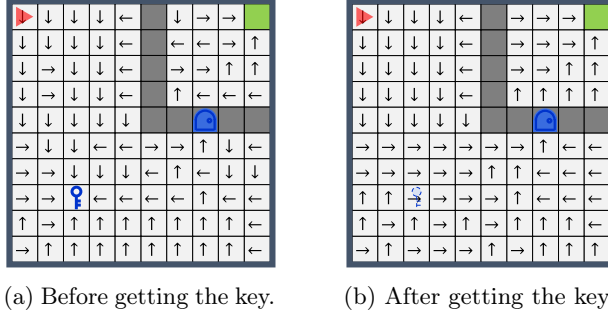


Figure 7: Actions yielding the highest knowledge rewards at each state in a new *2DMaze* task.

most states receive reasonable rewards that align with human understanding. This demonstrates the effectiveness of knowledge transfer, and with such dense rewards, the agent’s adaptation to new tasks is able to be well supported.

## 5.4 Effect of Sampling Weight

We conducted experiments to understand the effects of the information synchronization mechanism in the CenRA. Specifically, we compare the full CenRA model against three variants: (a) CenRA without the similarity weight  $w^{sim}$ , (b) CenRA without the performance weight  $w^{per}$ , and (c) CenRA without the entire sampling weight. To better illustrate the differences among tasks and highlight the role of sampling weights in task coordination and synchronization, we select the four-task domains, i.e., *2DMaze*, *3DPickup*, and *MujocoCar*. The comparison results are shown in Table 3.

Table 3: Comparison of CenRA with ablation of different batch sampling control weights.

Algo.	<i>2DMaze</i>				Var. ↓ ( $\times 10^{-2}$ )
	Maze #1	Maze #2	Maze #3	Maze #4	
CenRA	<b>0.89 ± 0.03</b>	0.91 ± 0.02	<b>0.92 ± 0.02</b>	<b>0.93 ± 0.02</b>	0.02
w/o $w^{sim}$	0.88 ± 0.03	<b>0.92 ± 0.02</b>	0.87 ± 0.04	0.82 ± 0.04	0.17
w/o $w^{per}$	0.76 ± 0.06	0.88 ± 0.03	0.82 ± 0.05	0.87 ± 0.02	0.28
w/o both	0.63 ± 0.05	0.83 ± 0.04	0.63 ± 0.08	0.80 ± 0.05	1.24

Algo.	<i>3DPickup</i>				Var. ↓ ( $\times 10^{-2}$ )
	Ball	Cube	Key	Health kit	
CenRA	<b>0.95 ± 0.02</b>	0.68 ± 0.09	<b>0.80 ± 0.06</b>	0.69 ± 0.07	1.57
w/o $w^{sim}$	0.82 ± 0.07	<b>0.70 ± 0.09</b>	0.70 ± 0.07	<b>0.89 ± 0.04</b>	0.89
w/o $w^{per}$	0.78 ± 0.07	0.40 ± 0.09	0.63 ± 0.08	0.44 ± 0.10	3.05
w/o both	0.81 ± 0.07	0.46 ± 0.06	0.48 ± 0.08	0.37 ± 0.08	3.80

Algo.	<i>MujocoCar</i>				Var. ↓ ( $\times 10^3$ )
	Target #1	Target #2	Target #3	Target #4	
CenRA	<b>588.2 ± 0.73</b>	<b>549.3 ± 0.64</b>	447.7 ± 0.67	<b>474.3 ± 0.66</b>	4.24
w/o $w^{sim}$	319.9 ± 0.59	486.8 ± 0.71	332.5 ± 0.70	260.9 ± 0.54	9.29
w/o $w^{per}$	320.9 ± 0.89	355.3 ± 0.68	344.1 ± 0.87	308.2 ± 0.72	0.46
w/o both	57.5 ± 0.35	257.0 ± 0.68	<b>677.3 ± 0.54</b>	77.6 ± 0.26	82.7

The results indicate that the two weights, which control the allocation of samples drawn from each policy agent’s experiences, mainly influence the overall learning performance. Specifically, the absence of sampling weight leads to unbalanced learning outcomes, which is observed by the increased variance in episodic

returns across four tasks. While the full CenRA model does not always achieve the lowest variance, it consistently outperforms the other three ablation models regarding overall system performance.

Both weights play essential roles in the information synchronization, with the performance weight  $w^{per}$  having a more important impact. It allows CRA to pay more attention to the policy agents that are underperforming or progressing slowly. This suggests that considering the overall learning performance of the multi-task system is also an important objective that CenRA seeks to achieve.

## 6 Discussion and Conclusion

We propose a novel framework named CenRA that innovatively integrates reward shaping into MTRL. The framework not only shares domain knowledge across tasks to improve learning efficiency but also effectively addresses the sparse-reward challenge. Specifically, the centralized reward agent functions as a knowledge pool, responsible for knowledge distillation and distribution across multiple tasks. Furthermore, our information synchronization mechanism mitigates knowledge distribution disparities across tasks, ensuring optimal system-wide performance. Experiments demonstrate that the dense knowledge rewards generated by the CRA efficiently guide the policy agents’ learning, leading to faster convergence compared to baseline methods. The CenRA also performs superiorly and robustly in transferring acquired knowledge to new tasks.

CenRA’s current limitation is its requirement for uniform state and action shapes across tasks. Future improvements could explore preprocessing techniques to adapt the framework for varying state and action shapes to broaden CenRA’s applicability. Additionally, the fixed trade-off between similarity weight and performance weight may not be ideal. A more flexible approach, potentially through adaptive regulation of these weights, could further enhance the framework. Besides, the performance weight might favor underperforming tasks, achieving overall balance, but potentially limiting the upper bound of top-performing tasks. This issue could necessitate a better mechanism for trade-offs.

## References

- Ammar, H. B., Eaton, E., Ruvoilo, P., and Taylor, M. (2014). Online multi-task learning for policy gradient methods. In *International conference on machine learning*, pages 1206–1214. PMLR.
- Aradi, S. (2020). Survey of deep reinforcement learning for motion planning of autonomous vehicles. *IEEE Transactions on Intelligent Transportation Systems*, 23(2):740–759.
- Bai, F., Zhang, H., Tao, T., Wu, Z., Wang, Y., and Xu, B. (2023). Picor: Multi-task deep reinforcement learning with policy correction. In *Proceedings of the AAAI Conference on Artificial Intelligence*, volume 37, pages 6728–6736.
- Bellemare, M., Srinivasan, S., Ostrovski, G., Schaul, T., Saxton, D., and Munos, R. (2016). Unifying count-based exploration and intrinsic motivation. *Advances in Neural Information Processing Systems*, 29.
- Burda, Y., Edwards, H., Storkey, A., and Klimov, O. (2018). Exploration by random network distillation. In *International Conference on Learning Representations*.
- Caruana, R. (1993). Multitask learning: A knowledge-based source of inductive bias<sup>1</sup>. In *Proceedings of the Tenth International Conference on Machine Learning*, pages 41–48. Citeseer.
- Chen, Z., Badrinarayanan, V., Lee, C.-Y., and Rabinovich, A. (2018). Gradnorm: Gradient normalization for adaptive loss balancing in deep multitask networks. In *International conference on machine learning*, pages 794–803. PMLR.
- Cheng, G., Dong, L., Cai, W., and Sun, C. (2023). Multi-task reinforcement learning with attention-based mixture of experts. *IEEE Robotics and Automation Letters*, 8(6):3812–3819.
- Chevalier-Boisvert, M., Dai, B., Towers, M., Perez-Vicente, R., Willems, L., Lahlou, S., Pal, S., Castro, P. S., and Terry, J. (2024). Minigrid & miniworld: Modular & customizable reinforcement learning environments for goal-oriented tasks. *Advances in Neural Information Processing Systems*, 36.
- D’Eramo, C., Tateo, D., Bonarini, A., Restelli, M., and Peters, J. (2020). Sharing knowledge in multi-task deep reinforcement learning. In *International Conference on Learning Representations*.
- Devidze, R., Kamalaruban, P., and Singla, A. (2022). Exploration-guided reward shaping for reinforcement learning under sparse rewards. *Advances in Neural Information Processing Systems*, 35:5829–5842.
- Devin, C., Gupta, A., Darrell, T., Abbeel, P., and Levine, S. (2017). Learning modular neural network policies for multi-task and multi-robot transfer. In *2017 IEEE international conference on robotics and automation (ICRA)*, pages 2169–2176. IEEE.
- Finn, C., Abbeel, P., and Levine, S. (2017). Model-agnostic meta-learning for fast adaptation of deep networks. In *International conference on machine learning*, pages 1126–1135. PMLR.
- Fujimoto, S., Hoof, H., and Meger, D. (2018). Addressing function approximation error in actor-critic methods. In *International conference on machine learning*, pages 1587–1596. PMLR.
- Haarnoja, T., Zhou, A., Abbeel, P., and Levine, S. (2018a). Soft actor-critic: Off-policy maximum entropy deep reinforcement learning with a stochastic actor. In *International Conference on Machine Learning*, pages 1861–1870. PMLR.
- Haarnoja, T., Zhou, A., Hartikainen, K., Tucker, G., Ha, S., Tan, J., Kumar, V., Zhu, H., Gupta, A., Abbeel, P., et al. (2018b). Soft actor-critic algorithms and applications. *arXiv preprint arXiv:1812.05905*.
- He, J., Li, K., Zang, Y., Fu, H., Fu, Q., Xing, J., and Cheng, J. (2024). Not all tasks are equally difficult: Multi-task deep reinforcement learning with dynamic depth routing. In *Proceedings of the AAAI Conference on Artificial Intelligence*, volume 38, pages 12376–12384.

- Hessel, M., Soyer, H., Espeholt, L., Czarnecki, W., Schmitt, S., and Van Hasselt, H. (2019). Multi-task deep reinforcement learning with popart. In *Proceedings of the AAAI Conference on Artificial Intelligence*, volume 33, pages 3796–3803.
- Hong, S., Yoon, D., and Kim, K.-E. (2021). Structure-aware transformer policy for inhomogeneous multi-task reinforcement learning. In *International Conference on Learning Representations*.
- Huang, S., Dossa, R. F. J., Ye, C., Braga, J., Chakraborty, D., Mehta, K., and AraÅšjo, J. G. (2022). Cleanrl: High-quality single-file implementations of deep reinforcement learning algorithms. *Journal of Machine Learning Research*, 23(274):1–18.
- Ji, J., Zhang, B., Zhou, J., Pan, X., Huang, W., Sun, R., Geng, Y., Zhong, Y., Dai, J., and Yang, Y. (2023). Safety gymnasium: A unified safe reinforcement learning benchmark. *Advances in Neural Information Processing Systems*, 36.
- Kober, J., Bagnell, J. A., and Peters, J. (2013). Reinforcement learning in robotics: A survey. *The International Journal of Robotics Research*, 32(11):1238–1274.
- Konda, V. and Tsitsiklis, J. (1999). Actor-critic algorithms. *Advances in neural information processing systems*, 12.
- Ladosz, P., Weng, L., Kim, M., and Oh, H. (2022). Exploration in deep reinforcement learning: A survey. *Information Fusion*, 85:1–22.
- Lample, G. and Chaplot, D. S. (2017). Playing fps games with deep reinforcement learning. In *Proceedings of the AAAI conference on artificial intelligence*, volume 31.
- Lan, S., Zhang, R., Yi, Q., Guo, J., Peng, S., Gao, Y., Wu, F., Chen, R., Du, Z., Hu, X., et al. (2023). Contrastive modules with temporal attention for multi-task reinforcement learning. *Advances in Neural Information Processing Systems*, 36.
- Luo, Z., Ma, H., Shi, D., and Gan, W.-S. (2024). Gfanc-rl: Reinforcement learning-based generative fixed-filter active noise control. *Available at SSRN 4837239*.
- Ma, H., Li, F., Lim, J. Y., Luo, Z., Vo, T. V., and Leong, T.-Y. (2025a). Catching two birds with one stone: Reward shaping with dual random networks for balancing exploration and exploitation. In *Forty-second International Conference on Machine Learning*. PMLR.
- Ma, H., Luo, Z., Vo, T. V., Sima, K., and Leong, T.-Y. (2025b). Highly efficient self-adaptive reward shaping for reinforcement learning. In *Thirteenth International Conference on Learning Representations*.
- Ma, H., Sima, K., Vo, T. V., Fu, D., and Leong, T.-Y. (2024a). Reward shaping for reinforcement learning with an assistant reward agent. In *Forty-first International Conference on Machine Learning*. PMLR.
- Ma, H., Vo, T. V., and Leong, T.-Y. (2023). Hierarchical reinforcement learning with human-ai collaborative sub-goals optimization. In *Proceedings of the 2023 international conference on autonomous agents and multiagent systems*, pages 2310–2312.
- Ma, H., Vo, T. V., and Leong, T.-Y. (2024b). Mixed-initiative bayesian sub-goal optimization in hierarchical reinforcement learning. In *Proceedings of the 23rd International Conference on Autonomous Agents and Multiagent Systems*, pages 1328–1336.
- Mavor-Parker, A., Young, K., Barry, C., and Griffin, L. (2022). How to stay curious while avoiding noisy tvs using aleatoric uncertainty estimation. In *International Conference on Machine Learning*, pages 15220–15240. PMLR.
- Memarian, F., Goo, W., Lioutikov, R., Niekum, S., and Topcu, U. (2021). Self-supervised online reward shaping in sparse-reward environments. In *2021 IEEE/RSJ International Conference on Intelligent Robots and Systems (IROS)*, pages 2369–2375. IEEE.

- Mguni, D., Jafferjee, T., Wang, J., Perez-Nieves, N., Song, W., Tong, F., Taylor, M., Yang, T., Dai, Z., Chen, H., et al. (2023). Learning to shape rewards using a game of two partners. In *AAAI Conference on Artificial Intelligence*, volume 37, pages 11604–11612.
- Mnih, V., Kavukcuoglu, K., Silver, D., Rusu, A. A., Veness, J., Bellemare, M. G., Graves, A., Riedmiller, M., Fidjeland, A. K., Ostrovski, G., et al. (2015). Human-level control through deep reinforcement learning. *Nature*, 518(7540):529–533.
- Mysore, S., Cheng, G., Zhao, Y., Saenko, K., and Wu, M. (2022). Multi-critic actor learning: Teaching rl policies to act with style. In *International Conference on Learning Representations*.
- Ostrovski, G., Bellemare, M. G., Oord, A., and Munos, R. (2017). Count-based exploration with neural density models. In *International Conference on Machine Learning*, pages 2721–2730. PMLR.
- Ouyang, L., Wu, J., Jiang, X., Almeida, D., Wainwright, C., Mishkin, P., Zhang, C., Agarwal, S., Slama, K., Ray, A., et al. (2022). Training language models to follow instructions with human feedback. *Advances in neural information processing systems*, 35:27730–27744.
- Parisotto, E., Ba, J., and Salakhutdinov, R. (2016). Actor-mimic: Deep multitask and transfer reinforcement learning. In *International Conference on Learning Representations*.
- Pathak, D., Agrawal, P., Efros, A. A., and Darrell, T. (2017). Curiosity-driven exploration by self-supervised prediction. In *International Conference on Machine Learning*, pages 2778–2787. PMLR.
- Rusu, A. A., Colmenarejo, S. G., Gulcehre, C., Desjardins, G., Kirkpatrick, J., Pascanu, R., Mnih, V., Kavukcuoglu, K., and Hadsell, R. (2016). Policy distillation. In *International Conference on Learning Representations*.
- Shinn, N., Cassano, F., Gopinath, A., Narasimhan, K., and Yao, S. (2023). Reflexion: Language agents with verbal reinforcement learning. *Advances in Neural Information Processing Systems*, 36:8634–8652.
- Sodhani, S., Zhang, A., and Pineau, J. (2021). Multi-task reinforcement learning with context-based representations. In *International Conference on Machine Learning*, pages 9767–9779. PMLR.
- Sorg, J., Lewis, R. L., and Singh, S. (2010a). Reward design via online gradient ascent. *Advances in Neural Information Processing Systems*, 23.
- Sorg, J., Singh, S. P., and Lewis, R. L. (2010b). Internal rewards mitigate agent boundedness. In *International Conference on Machine Learning*, pages 1007–1014.
- Sun, L., Zhang, H., Xu, W., and Tomizuka, M. (2022). Paco: Parameter-compositional multi-task reinforcement learning. *Advances in Neural Information Processing Systems*, 35:21495–21507.
- Tang, H., Houthooft, R., Foote, D., Stooke, A., Xi Chen, O., Duan, Y., Schulman, J., DeTurck, F., and Abbeel, P. (2017). # exploration: A study of count-based exploration for deep reinforcement learning. *Advances in Neural Information Processing Systems*, 30.
- Teh, Y., Bapst, V., Czarnecki, W. M., Quan, J., Kirkpatrick, J., Hadsell, R., Heess, N., and Pascanu, R. (2017). Distral: Robust multitask reinforcement learning. *Advances in neural information processing systems*, 30.
- Vaswani, A., Shazeer, N., Parmar, N., Uszkoreit, J., Jones, L., Gomez, A. N., Kaiser, Ł., and Polosukhin, I. (2017). Attention is all you need. *Advances in neural information processing systems*, 30.
- Vuong, T.-L., Nguyen, D.-V., Nguyen, T.-L., Bui, C.-M., Kieu, H.-D., Ta, V.-C., Tran, Q.-L., and Le, T.-H. (2019). Sharing experience in multitask reinforcement learning. In *International Joint Conference on Artificial Intelligence*, pages 3642–3648.

- Wan, M., Gangwani, T., and Peng, J. (2020). Mutual information based knowledge transfer under state-action dimension mismatch. In *Conference on Uncertainty in Artificial Intelligence*, pages 1218–1227. PMLR.
- Xu, T., Li, Z., and Ren, Q. (2024). Meta-reinforcement learning robust to distributional shift via performing lifelong in-context learning. In *Proceedings of the 41st International Conference on Machine Learning*, volume 235 of *Proceedings of Machine Learning Research*, pages 55112–55125. PMLR.
- Xu, Z., Wu, K., Che, Z., Tang, J., and Ye, J. (2020). Knowledge transfer in multi-task deep reinforcement learning for continuous control. *Advances in Neural Information Processing Systems*, 33:15146–15155.
- Yang, R., Xu, H., Wu, Y., and Wang, X. (2020). Multi-task reinforcement learning with soft modularization. *Advances in Neural Information Processing Systems*, 33:4767–4777.
- Yang, Z., Merrick, K. E., Abbass, H. A., and Jin, L. (2017). Multi-task deep reinforcement learning for continuous action control. In *International Joint Conference on Artificial Intelligence*, volume 17, pages 3301–3307.
- Yin, H. and Pan, S. (2017). Knowledge transfer for deep reinforcement learning with hierarchical experience replay. In *Proceedings of the AAAI Conference on Artificial Intelligence*, volume 31.
- Yu, T., Kumar, S., Gupta, A., Levine, S., Hausman, K., and Finn, C. (2020a). Gradient surgery for multi-task learning. *Advances in Neural Information Processing Systems*, 33:5824–5836.
- Yu, T., Quillen, D., He, Z., Julian, R., Hausman, K., Finn, C., and Levine, S. (2020b). Meta-world: A benchmark and evaluation for multi-task and meta reinforcement learning. In *Conference on robot learning*, pages 1094–1100. PMLR.
- Zeng, S., Anwar, M. A., Doan, T. T., Raychowdhury, A., and Romberg, J. (2021). A decentralized policy gradient approach to multi-task reinforcement learning. In *Uncertainty in Artificial Intelligence*, pages 1002–1012. PMLR.



## A Mutli-Task Experimental Configurations

We conduct experiments in four domains with multiple tasks: *Meta-World*, *2DMaze*, *3DPickup*, and *MujocoCar*. The detailed configurations of each task are illustrated in Figure 8. The *Meta-World* tasks illustration is adapted from (Yu et al., 2020b).

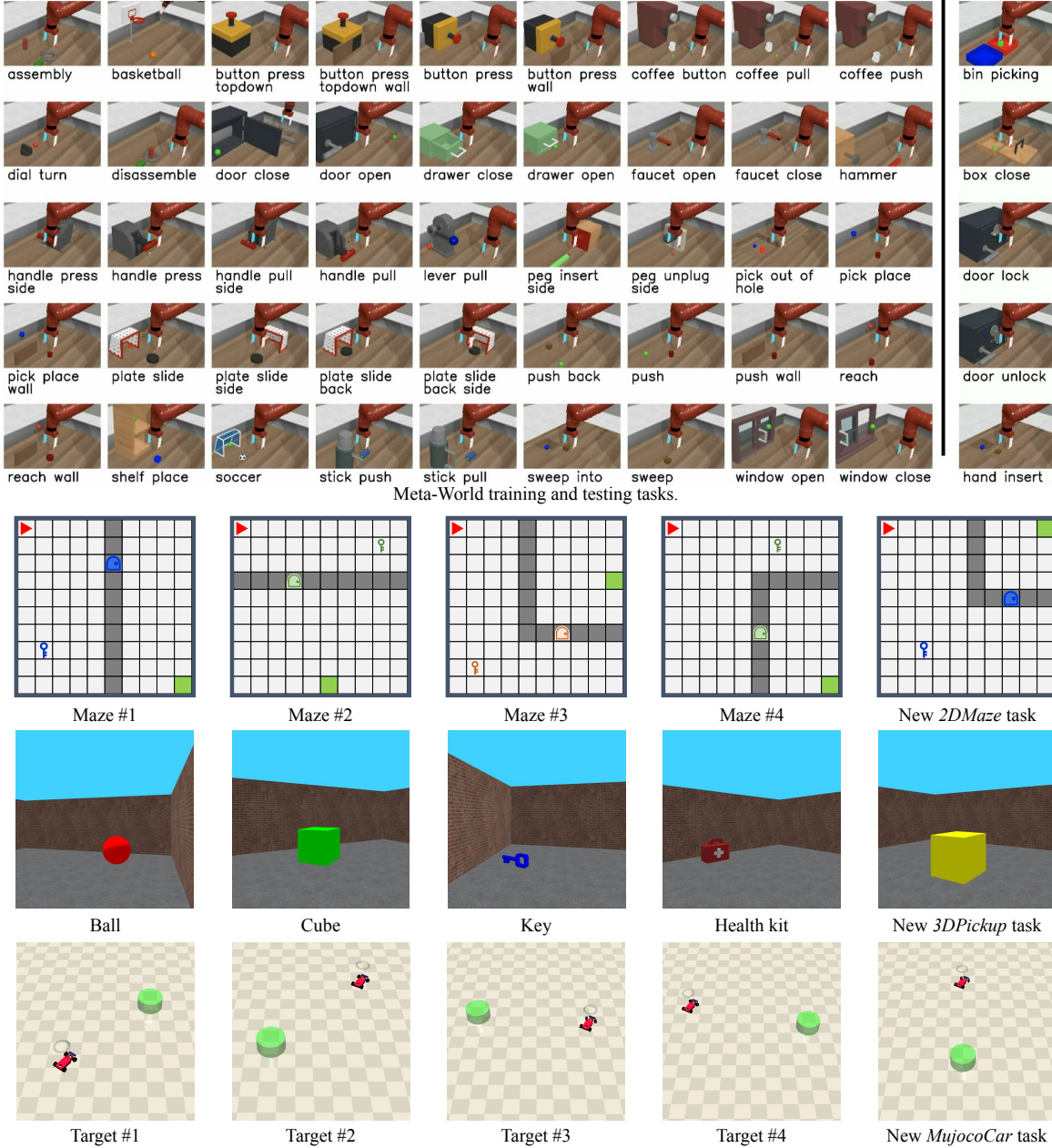


Figure 8: Illustration of multiple tasks in different domains in our experiments.

## B Experimental Configurations

### B.1 Network Structures

Figure 9 illustrates the structures of all networks employed in our experiments.

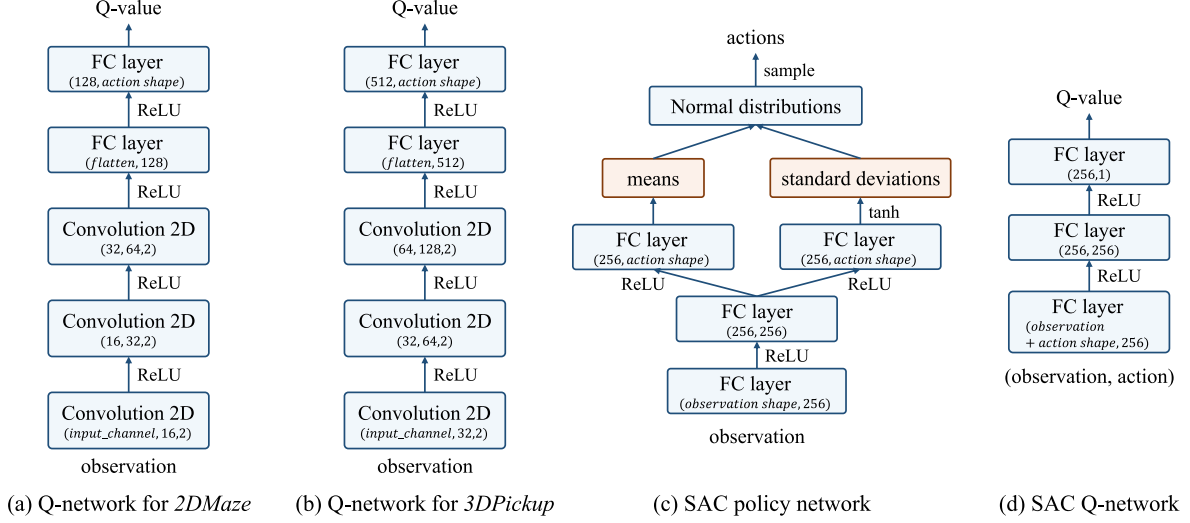


Figure 9: The structures of neural networks in our implementation.

### B.2 Computing Resources

The experiments in this paper were conducted on a computing cluster, with the detailed hardware configurations listed in Table 4.

Table 4: The computing resources used in the experiments.

Component	Specification
Operating System (OS)	Ubuntu 20.04
Central Processing Unit (CPU)	2x Intel Xeon Gold 6326
Random Access Memory (RAM)	256GB
Graphics Processing Unit (GPU)	1x NVIDIA A100 20GB
Brand	Supermicro 2022

### B.3 Hyperparameters

We have observed that CenRA demonstrated high robustness and was not sensitive to hyperparameter choices. Table 5 shows the hyperparameters we used in all the experiments.

Table 5: The hyperparameters of CenRA used in our experiments.

Module	Hyperparameters	Values
Centralized Reward Agent $\mathcal{A}^{rwd}$	discounted factor $\gamma$	0.99
	batch size	256
	actor module learning rate	$3 \times 10^{-4}$
	critic module learning rate	$1 \times 10^{-3}$
	policy networks update frequency (steps)	2
	target networks update frequency (steps)	1
	target networks soft update weight $\tau$	$5 \times 10^{-3}$
	burn-in steps	5000
Policy Agent $\mathcal{A}_i^{pol}$ (DQN Agent)	knowledge reward weight $\lambda$	0.5
	discounted factor $\gamma$	0.99
	replay buffer size $ \mathcal{D}_i $	$1 \times 10^6$
	batch size	128
	burn-in steps	10000
Policy Agent $\mathcal{A}_i^{pol}$ (SAC Agent)	knowledge reward weight $\lambda$	0.5
	discounted factor $\gamma$	0.99
	replay buffer size $ \mathcal{D}_i $	$1 \times 10^6$
	batch size	256
	actor module learning rate	$3 \times 10^{-4}$
	critic module learning rate	$1 \times 10^{-3}$
	SAC entropy term factor $\alpha$ learning rate	$1 \times 10^{-4}$
	policy networks update frequency (steps)	2
	target networks update frequency (steps)	1
	target networks soft update weight $\tau$	$5 \times 10^{-3}$
	burn-in steps	10000